Phylogeography of the Teiid Lizard *Kentropyx calcarata* and the Sphaerodactylid *Gonatodes humeralis* (Reptilia: Squamata): Testing A Geological Scenario for the Lower Amazon–Tocantins Basins, Amazonia, Brazil

Author(s) :Teresa C. S. Avila-Pires, Daniel G. Mulcahy, Fernanda P. Werneck, and Jack W., Sites, Jr.
Source: Herpetologica, 68(2):272-287. 2012.
Published By: The Herpetologists' League
DOI: http://dx.doi.org/10.1655/HERPETOLOGICA-D-11-00021.1
URL: http://www.bioone.org/doi/full/10.1655/HERPETOLOGICA-D-11-00021.1

Herpetologica, 68(2), 2012, 272–287

PHYLOGEOGRAPHY OF THE TEIID LIZARD *KENTROPYX CALCARATA* AND THE SPHAERODACTYLID *GONATODES HUMERALIS* (REPTILIA: SQUAMATA): TESTING A GEOLOGICAL SCENARIO FOR THE LOWER AMAZON–TOCANTINS BASINS, AMAZONIA, BRAZIL

TERESA C. S. AVILA-PIRES[1,4], DANIEL G. MULCAHY[2,3], FERNANDA P. WERNECK[2], AND JACK W. SITES, JR.[2]

[1]*Museu Paraense Emílio Goeldi/CZO, C.P. 399, 66017-970, Belém, Pará, Brazil*
[2]*Department of Biology and Bean Life Science Museum, Brigham Young University, Provo, UT 84602, USA*

ABSTRACT: In spite of Amazonia's large biodiversity, we still understand relatively little about how it evolved. Phylogeographic studies help us to understand the spatial and temporal context in the diversification of organisms, but only a few such studies have been done in Amazonia, where regional and local variation exists that may have been influenced by different events or similar events at different times. Here we test whether, and to what degree, the phylogeographic structure of faunal elements reflects a recently proposed geological scenario for the establishment of the lower Amazon–Tocantins basins in eastern Amazonia. We test an area cladogram that assumes that the Amazon River represents the first potential barrier (≥3.6 million years ago [mya]), followed by an east–west separation south of the Amazon caused by the paleo-Tocantins River (~2.5 mya), and most recently by the shift of the lower Tocantins eastward to its present course (~6000–8000 yr ago). We examined mtDNA (~520 base-pairs [bp] of *16S*, 815 bp of *cytochrome b*) of two widely distributed and distantly related lizard species, *Gonatodes humeralis* (Sphaerodactylidae) and *Kentropyx calcarata* (Teiidae). The phylogeographic structure of *G. humeralis* indicates that the species is characterized by deep splits between localities, preventing us from recovering well-supported relationships between populations. *Kentropyx calcarata* haplotype networks and our Bayesian mtDNA tree identify a number of clades that we compare through an AMOVA. The overall phylogeny of *K. calcarata* was partially congruent with the geological scenario, but some unforeseen relationships were also recovered. Our results reinforce the potential of phylogeographic studies to help understand the recent evolution of Amazonia, and at the same time point to the necessity of refined sampling and the use of multiple molecular markers in such studies.

RESUMO: Apesar da grande biodiversidade existente na Amazônia, ainda conhecemos relativamente pouco como ela evoluiu. Estudos filogeográficos ajudam a entender o contexto espacial e temporal da diversificação dos organismos, mas apenas poucos estudos desse tipo foram feitos na Amazônia, que apresenta variações locais e regionais que podem ter sido influenciadas por diferentes eventos, ou por eventos similares em tempos distintos. Testamos aqui se, e em que grau, a estrutura filogeográfica de elementos da fauna reflete um cenário geológico proposto recentemente para a bacia do baixo Amazonas–Tocantins, na Amazônia oriental. Testamos um cladograma de área que assume que o Rio Amazonas representa a primeira barreira potencial (≥ 3.6 milhões de anos atrás, mya), seguida por uma separação leste-oeste ao sul do Rio Amazonas causada pelo paleo-Tocantins (~2,5 mya), e mais recentemente pelo deslocamento em direção leste do baixo curso do Rio Tocantins (~6–8 mil anos atrás). Examinamos o mtDNA (~520bp de *16S* e 815 bp de *citocromo b*) de duas espécies de lagartos amplamente distribuídas e não proximamente relacionadas, *Gonatodes humeralis* (Sphaerodactylidae) e *Kentropyx calcarata* (Teiidae). A estrutura filogeográfica de *G. humeralis* indica tratar-se de uma espécie caracterizada por separações profundas entre localidades, impedindo-nos de recuperar, com bom suporte estatístico, a relação entre elas. Em *K. calcarata*, as redes de haplótipos e a árvore Bayesiana obtidas a partir do mtDNA apontaram para uma série de clados que foram comparados através de uma AMOVA. As relações filogenéticas obtidas para essa espécie foram parcialmente congruentes com o cenário geológico, mas algumas relações inesperadas também foram recuperadas. Nossos resultados reforçam o potencial de estudos filogeográficos em ajudar a entender a evolução recente da Amazônia, e apontam simultaneamente para a necessidade de amostragens refinadas e o uso de marcadores moleculares múltiplos em tais estudos.

Key words: Amazonia; *Gonatodes humeralis*; *Kentropyx calcarata*; mt-DNA; Phylogeography

AMAZONIA is generally considered to harbor the richest terrestrial fauna and flora on Earth (Mittermeier et al., 2003), and multiple alternative hypotheses have been presented to

[3] PRESENT ADDRESS: Smithsonian Institution, Museum Support Center, Suitland, MD 20746, USA
[4] CORRESPONDENCE: e-mail, avilapires@museu-goeldi.br

explain the diversification of its biota (Moritz et al., 2000; Antonelli et al., 2010; Hoorn et al., 2010). Some of these hypotheses (e.g., "riverine barrier"; Wallace, 1852) have been investigated with phylogeographic approaches in some taxa (see below), but the majority remain untested. Studies of this nature are in part limited by the size and scale of the region, and by the difficulty of adequate sampling to permit rigorous testing of alternative hypotheses (summarized in Table 1 of Moritz et al., 2000). For most taxa, Amazonia remains "terra incognita" and its biota present many examples of Linnean and Wallacean "shortfalls" (Lomolino, 2004)—inadequate knowledge of species' boundaries and distributions, respectively. These shortfalls constraint more detailed studies of both evolutionary mechanisms that generate and maintain biodiversity and the application of such knowledge to conservation planning (e.g., Silva et al., 2005; Fouquet et al., 2007).

Phylogeographic studies may help to clarify the spatial and temporal context of diversification of organisms in Amazonia, which can be compared with specific geological scenarios (Moritz et al., 2000). Some studies on vertebrates (e.g., Silva and Patton, 1998; Aleixo, 2004; Geurgas and Rodrigues, 2009) have been conducted recently with this aim, but results are still contradictory and many more studies are needed before we can understand how this complex biota has evolved. One aspect that contributes to this complexity is that the Amazon region is not uniform and its formation did not happen as a single event. Local and regional variation exists, and different areas may have been influenced by different events or similar events at different times, and therefore experienced different environments throughout their histories (Hoorn et al., 2010). Therefore, it is necessary to examine these different regional histories in detail, in order to understand Amazonia as a whole.

A number of hypotheses have been proposed to explain the richness and distribution of present Amazonian biota. They do not necessarily mutually exclude each other, and each may have played a role in shaping present biota in different times or areas within the region. For instance, western Amazonia was dominated during much of the Miocene by the Pebas mega-wetland, which isolated large tracks of land, especially the western and eastern portions of northern South America (Wesselingh et al., 2010). By Late Miocene–Pliocene, the modern Amazon River system was established (Figueiredo et al., 2009; Wesselingh et al., 2010), which may have triggered speciation events in part of the fauna, as proposed by the Riverine hypothesis (Wallace, 1852; Ayres and Clutton-Brock, 1992). Such modifications in the fluvial system were directly linked to the elevation of the Andes, which was accompanied by several tectonic events across the entire region that may have caused additional vicariance events. More recently, during the Quaternary, climatic oscillations may have promoted local and regional vegetation shifts, which potentially affected the population dynamics of many species by retracting or expanding distributional extents. The Pleistocene refugia hypothesis (Haffer, 1969; Vanzolini and Williams, 1970) proposed an extreme scenario where the Amazon forest became restricted to several refugia, surrounded by savannah vegetation, during the coldest or driest periods. Haffer later (1992, 2001) acknowledged the possibility of a broader spectrum of situations without denying the importance of climatic cycles on the diversification of Amazonian fauna. It is clear, therefore, that no single hypothesis explains the diversification of Amazonian fauna. It is essential to look at specific scenarios, in the appropriate time span, to try to understand their roles in shaping parts of the biota.

New data on the recent geological history of the lower Tocantins River–Marajó Island in eastern Amazonia (Rossetti and Valeriano, 2007; Rossetti and Góes, 2008), as well as on the Amazon River (Figueiredo et al., 2009), have clarified some of the most recent geological events that shaped the modern Amazon drainage basin, and have provided a better idea about the ages of such events. According to Figueiredo et al. (2009), during the Early Miocene an ancestral Amazon River was restricted to eastern Amazonia, while sediments of Andean origin started to reach the current mouth of the Amazon by Late Miocene (11.8–11.3 mya), with an increase in sedimentation rates between 6.8–2.4 mya. Latrubesse et al. (2010), on the other hand, argued that the Amazon system only acquired

its present configuration during the early Pliocene, thus at least partially in agreement with the increase in sedimentation rates observed by Figueiredo et al. (2009). Whatever the exact age, we can consider that there has been a barrier separating the fauna north and south of the river since at least the early Pliocene (5.3–3.6 mya).

Rossetti and Valeriano (2007) have also shown that the Marajó Island, at the mouth of the Amazon and Tocantins rivers, was formed as recently as the Middle to Late Holocene, by a sequence of tectonic events that first detached the southeastern part of the island when the lower course of the Tocantins River changed from a south–north position to a more southwest–northeast position. This first event is hypothesized to have occurred by Late Pleistocene or Early Holocene (~6000–8000 yr BP). Later the present Pará River was created by a new geological fault, isolating what is presently known as the Marajó Island. There are no studies estimating the age of the paleo-Tocantins, with a south–north position and cutting through what is today the Marajó Island, but Rossetti and Valeriano (2007) showed that the area is covered by sediments of Plio–Pleistocene or Pleistocene ages. Taking this into consideration, we may assume that the paleo-Tocantins existed since ~2.5 mya, at the Pliocene–Pleistocene boundary. Summarizing the above information, the Amazon River represents the first potential faunal barrier in the study area, followed by an east–west separation south of the Amazon due to the paleo-Tocantins River, and most recently by the shift of the lower Tocantins eastward to its present course (Fig. 1). This latter event separated the Marajó Island from the area east of the Tocantins, even though the complete isolation of the Marajó Island occurred only by Middle to Late Holocene with formation of the Pará River.

We herein use the above regional model to predict expected spatial phylogeographic patterns of two widely distributed lizard species, *Gonatodes humeralis* (Guichenot, 1855), Sphaerodactylidae, and *Kentropyx calcarata* (Spix, 1825), Teiidae. Assuming that populations track the geological events with some fidelity, we could expect to find congruence between the area cladogram in Fig. 1B and the phylogeographic relationships among intraspecific populations. We used the mitochondrial *cytochrome b* and *16S* genes to investigate whether, and to what degree, phylogeographic structure of these lizards reflect the sequence of geomorphological events responsible for the establishment of the lower Tocantins River–Marajó Island in eastern Amazonia. Recent studies suggest that both

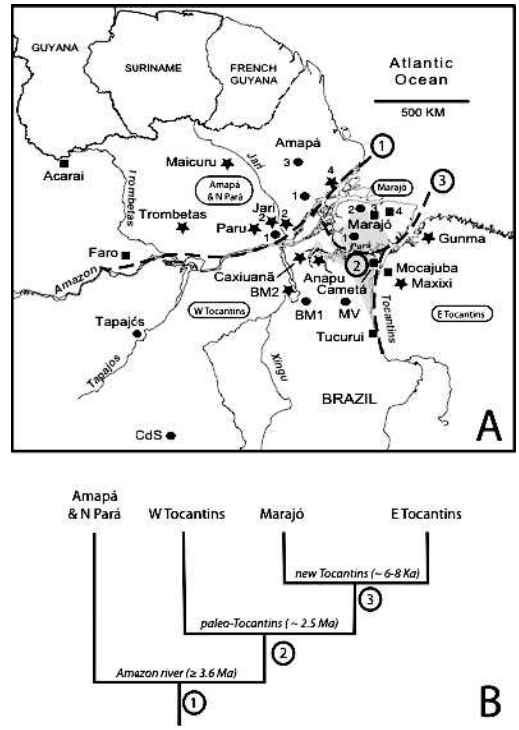

FIG. 1.—Sampled localities and hypothesis of area relationships. A—Map of eastern Amazonia showing the localities from which tissue samples were analyzed in this study (circles = *Kentropyx calcarata*; squares = *Gonatodes humeralis*; stars = both species). The four main areas considered in the study and represented in the area cladogram in Fig. 1B are shown and separated by dashed lines, with the names in oval circles. Numbers within circles correspond to the nodes in Fig. 1B. Area in light gray represents the approximate area covered by post-Barreiras sediments, which are hypothesized to have been deposited by the paleo-Tocantins (Rossetti and Valeriano, 2007). River names are in italicized gray font, and locality details are in Appendix I. B—Area cladogram hypothesized on basis of geologic data, considering the areas (1) north of the Amazon River (Amapá and N Pará), (2) Marajó Island, (3) west, and (4) east of Tocantins River. At each node the barrier that separated two areas or group of areas, and the approximate age for which there are evidences of its existence, are presented. See text for details.

target species have diversified at least since the Pliocene, when western (Peru and Ecuador) and eastern (Guyana and Pará) populations of *G. humeralis* (Gamble et al., 2008), and northern (Guyana) and southern (Mato Grosso, Brazil) populations of *K. calcarata* (Werneck et al., 2009) started to diverge from each other.

Both species are found in primary and secondary forest, but *G. humeralis* is more tolerant of disturbed areas (such as urban parks). *Kentropyx calcarata* is a heliothermic lizard that actively forages in the leaf litter and on fallen branches and trees close to or in sunny spots within the forest, while *G. humeralis* is active in the shade on tree trunks at several heights, but typically up to 2 m above ground (Avila-Pires, 1995; Vitt et al., 1997, 2000). Also, both species are more widely distributed than is represented by the geographical focus of our study; *K. calcarata* occurs in eastern and central Amazonia, in Guyana, Suriname, French Guiana, Brazil, and Bolivia, and in Brazil it is found also in forested areas of the northern and western parts of the Cerrado region, and in parts of the Atlantic forest. *Gonatodes humeralis* occurs throughout Amazonia and surrounding lowland regions, including coastal Venezuela and the islands of Trinidad and Tobago to the north, and the north-northwestern portion of the Brazilian Cerrado region to the south (Avila-Pires, 1995; Nogueira, 2006). Given the logistical issues of sampling such widely distributed species, we emphasize the exploratory nature and regional focus of this study and only test a single biogeographic hypothesis about a particular region of Amazonia. Our sampling is, however, adequate to test phylogeographic histories in the regional context of the lower Amazon–Tocantins basins.

Materials and Methods

Our study is based on 67 samples of *K. calcarata* from 20 localities in the states of Pará and Amapá, Brazil, and 56 samples of *G. humeralis* from 17 localities in these states (Fig. 1A; Appendix I). Tissues (muscle and liver) were preserved in ethanol, and voucher specimens were deposited in the collection of the Museu Paraense Emílio Goeldi (MPEG).

Genomic DNA was extracted from muscle or liver using the Qiagen DNeasy Blood and Tissue kit. Polymerase chain reaction (PCR) was performed for the mtDNA *cytochrome b* gene (*cyt b*) using the primers Glu (5′-TGA CTT GAA RAA CCA TCG TTG-3′) or IgCytb_F2 (5′-CCA CCG TTG TTA TTC AAC TAC-3′) and CB3-H (5′-GGC AAA TAG GAA RTA TCA TTC-3′), whereas those for *16S* were performed using primers 16Sar (5′-CGC CTG TTT ATC AAA AAC AT-3′) and 16Sbr (5′-CCG GTC TGA ACT CAG ATC ACG T-3′). Profiles for PCR, for both *cyt b* and *16S*, were: initial denaturation for 2:45 min at 94°C, followed by 35 cycles of 0:15 s of melting at 94°C, 1 min of annealing at a maximum temperature between 45°C and 51°C (with a decrease of 0.3°C at each cycle), and elongation for 1 min at 72°C, with a final elongation of 7 min at 72°C. The PCRs were conducted in 12-μL reactions, with TaKaRa *HS* Kit (hot start), buffer, and dNTPs included and primers at 10-μM concentration. Sequences were obtained for both directions using PCR primers and BigDye™ version 2.0 in reactions of 12-μL total volume following manufacturer's protocols. Sequence reaction products were purified with Sephadex (Sigma; St. Louis, MO) and run on an ABI 3730xl DNA Analyzer at BYU.

Sequences were edited and assembled using Sequencher 4.9 (Gene Codes Corporation) and aligned using MacClade 4.08 (Maddison and Maddison, 2005). In the case of *cyt b*, sequences were translated to amino acids to confirm alignment. The *16S* alignments were done by eye to maximize base-pair identity in conserved blocks; these sequences contained very few gaps (up to four 1–2-base-pair gaps in each taxon). Sequences of both genes were concatenated for subsequent analyses. All sequences generated for this project were deposited in GenBank (JQ639488–JQ639739).

Haplotype networks were generated in TCS 1.21 (Clement et al., 2000) using 95% and 90% parsimony connection limits. The same program was used to determine the number of unique haplotypes and the distribution of shared haplotypes. PAUP* 4.0b10 (Swofford, 2000) was used to calculate an average, uncorrected pairwise sequence divergence

between unique haplotypes for the major clades recovered within each species. MrModeltest 3.06 (Posada and Crandall, 1998) was used to select the nucleotide substitution models separately for *16S* and first, second, and third position codons of *cyt b*, under the Akaike information criterion (AIC), which was then employed in PAUP* to calculate corrected pairwise sequence divergence for the entire data set. Bayesian analyses were conducted using Parallel MrBayes @ BioHPC (http://cbsuapps.tc.cornell.edu/mrbayes.aspx), using the same partitions and models selected under the AIC, and were run for 10 million generations. Two runs were made simultaneously and stationarity was measured by the average standard deviation of split frequencies (ASDSF) and by visualization of log-likelihood scores plotted against generations using the program Tracer v1.4.1 (Rambaut and Drummond, 2007); mean, standard error of the mean, and effective sample size (ESS) are presented for the combined runs (obtained from Tracer v1.5). Post burn-in samples were used to estimate the posterior probability values, branch lengths, and topologies for each species. Trees sampled during the burn-in period were discarded, the remaining trees were used to construct a 50% majority-rule consensus tree, and posterior probabilities were calculated for each node. Bayesian trees were rooted with outgroups *Kentropyx striata* (AP304; for *K. calcarata*) and *G. annularis* (MPEG26672, MPEG26678; for *G. humeralis*). In the latter case, we also used a partial sequence downloaded from GenBank (Geurgas and Rodrigues, 2009; GenBank numbers DQ104101 [*16S*], DQ104133 [*cyt b*]), of *G. humeralis* (MTR 10015) from the lower Aripuanã River (Brazilian state of Amazonas). This sequence provided a more closely related outgroup, after preliminary analyses showed that all focal samples were more closely related to each other than they were to this specimen.

We conducted maximum-likelihood (ML) analyses on the combined *16S* and *cyt b* data sets for each species group using RAxML v7.0.4 (Stamatakis et al., 2005) with the rapid hill-climbing algorithm (Stamatakis et al., 2008). Searches were based on four partitions for each group (*16S* and each codon for *cyt b*) under the GTR-GAMMAI (GTR +I + Γ) model of nucleotide substitutions, 1000 bootstrap inferences, and 25 discrete GAMMA rate categories. *Kentropyx striata* and *G. annularis* (same specimens mentioned above) were used as outgroups. Bootstrap values ≥70% were considered well-supported (Hillis and Bull, 1993).

To verify our hypotheses of area relationships, we performed analyses of molecular variance (AMOVA; Arlequim 3.1; Excoffier et al., 2005), first grouping populations geographically according to the four areas shown in Fig. 1 (Amapá and north of Pará; Marajó; west of Tocantins River; and east of Tocantins River); and then within the well-supported clades obtained in the Bayesian analysis. Pairwise geographic and genetic distances were also compared using a Mantel test, through the Isolation-by-Distance Web Server (Jensen et al., 2005), with 10,000 randomizations. If our hypotheses that phylogeographic relationships within both species are congruent with the depicted area cladogram are correct, we should expect to find, in each species, less genetic variation within geographic groups than between them. Larger genetic variation between, rather than within, geographic groups would indicate greater isolation between, rather than within, the a priori defined geographic regions. This would indicate events in the history of the species that had different causes other than the geological events here considered, or that those events have not affected the species' recent phylogeographic histories. Because only one locality can be represented by a single sample in this analysis and we had multiple localities with only one sample each, a few localities (Gunma, Monte Verde and Tapajós in *K. calcarata*; Amapa 2, Faro, Maxixi and Belo Monte 2 in *G. humeralis*) were excluded from the Mantel test.

We calculated coalescent estimators of genetic diversity and demographic parameters to explore historical factors that may account for the observed differences on the phylogeographic structures between the two species. We used Migrate-n v 3.2.15 (Beerli and Palczewski, 2010) to estimate the diversity parameter (θ_{sites}); we implemented two independent maximum-likelihood runs with 20

short chains and 10 long chains, for 4000 and 40,000 generations, a burn-in of 40,000 steps, and starting parameters for the calculations derived from an F_{ST}-like calculation (Beerli and Palczewski, 2010). We calculated the diversity parameter (θ per sequence), nucleotide diversity per site (Pi), average net nucleotide differences (mean D_a) across localities represented by more than two individuals sampled, Tajima's D (Tajima, 1996), and Fay and Wu's *Hs* (Fay and Wu, 2000) tests to detect population expansion; and respective significance levels with 10,000 coalescent simulations using DnaSP (Rozas et al., 2003). Overall, significant negative values of these last two tests are consistent with a demographic history of recent population rapid expansion, whereas significantly positive values suggest that a population has undergone decrease in size (e.g., genetic bottleneck), and values that do not significantly differ from zero suggest population stability. We calculated the effective population sizes for each species assuming $\theta = 2Ne\mu$ (mtDNA, haploid), the estimates of theta (θ_{sites}), and based on the mtDNA substitution rate of 0.65% changes per million yr as derived by Macey et al. (1998) and widely employed, particularly for squamate reptiles. Although substitution rates may vary among families, the adopted substitution rate is very close to the mean rate of 0.53% changes per million yr calculated for lizard families in a recent comparative study (Eo and DeWoody, 2011).

Results

Kentropyx calcarata

In *K. calcarata,* the combined *16S–cyt b* alignment had 1338 base-pairs (519 bp of *16S*, 819 bp of *cyt b*). Of the 67 samples analyzed, 52 distinct haplotypes were found and linked into six independent networks when the TCS parsimony connection limit was set at 95%, and three networks when connection limit was 90%, plus one isolated haplotype (MPEG22297; supplemental material Fig. S1; available online). All haplotypes are restricted to a single locality, with the exception of a shared haplotype between Maicuru and Paru, both in the state of Pará north of the Amazon.

Figure 2 presents the Bayesian mtDNA tree recovered for the 52 unique *K. calcarata* haplotypes, with clades supported by moderate to high posterior probabilities identified (ASDSF = 0.004; generation/–lnL plots leveled off at ~500,000 generations, with burn-in made at 1000 trees; mean and SE of combined runs = −4030.09 ± 0.16, ESS = 4374.24). Four geographically cohesive clades are supported at values of $P = 1.0$ (Ia, Ib, Id, and Ie in Fig. 2), with two others at P of 0.97 and 0.93 (II and IIIa, respectively), and three geographically cohesive clades at $P = 0.84$ (Ic, IIIb, and If). When these are mapped onto the geographic localities (Fig. 3), the four most strongly supported clades (those with $P = 1.0$) include the following groups: (1) clade Ia—four localities north of the Amazon River, three of them in the state of Amapá (east of the Jari River), one just across the state border, in Pará (west of the Jari River); (2) clade Ib—four localities south of the main Amazon River, including two on Marajó Island and two just south and east of the mouth of the Tocantins River; (3) clade Id—two widely separated localities south of the Amazon and between the Tapajós and Xingu rivers; and (4) clade Ie—two localities (Caxiuanã and Trombetas) on opposite sides of the Amazon River (Fig. 3).

At a more inclusive level, clade II ($P = 0.97$) includes clades Ia and Ib north and south of the mouth of the Amazon River, respectively; note that Marajó localities are close to the "paleo-Tocantins" river channel and west of the mouth of the present Tocantins River. Clade IIIa ($P = 0.93$) includes clade II and clade Ic ($P = 0.84$); the latter is south of the Amazon but west of the Tocantins River (Fig. 3). Lastly, also at $P = 0.84$ level of support, we identified: (1) clade IIIb—which includes clade Id and a third locality on the west bank of the Tapajos River; and (2) clade If—which includes three localities in the state of Pará north of the Amazon River, of which one has haplotypes also in clade Ia (Fig. 3). In summary, Fig. 3 geographically illustrates the following nested patterns: (IIIa (Ic + II [Ia + Ib])) and (IIIb (Id)); at one node deeper, these two groups are then grouped again (IIIa + IIIb) but at a relatively low level of support ($P = 0.71$; Fig. 2). The remaining two clades, Ie and If, show little nesting of localities within each,

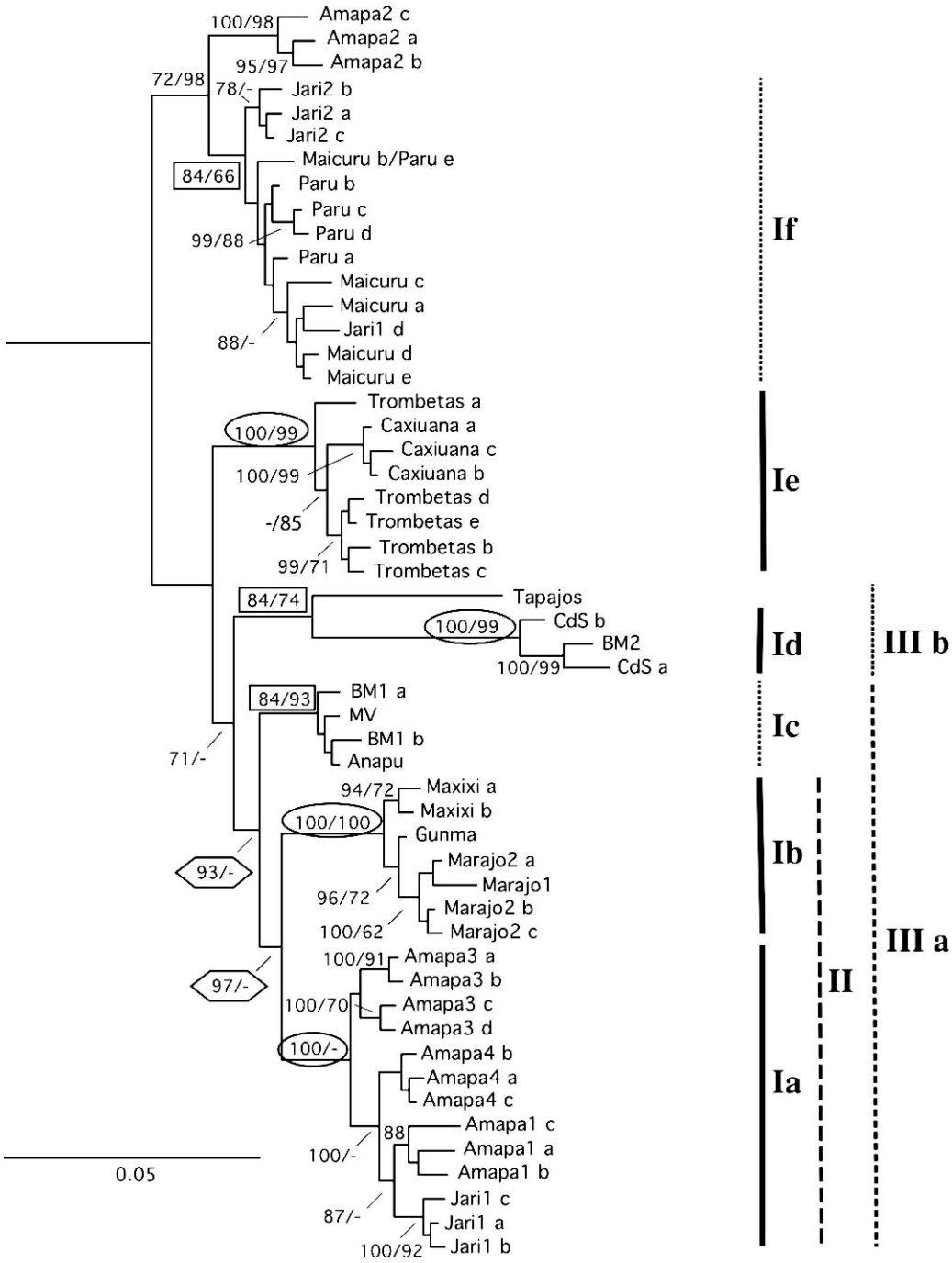

FIG. 2.—Bayesian consensus tree of concatenated *cyt b* and *16S* obtained for the samples of *Kentropyx calcarata*. Numbers at nodes represent posterior probabilities ≥70%/ML bootstrap values ≥50%. Haplotype terminals were replaced by their localities of origin followed by a letter (when more than one haplotype per locality) that identifies the specimen(s) with that haplotype in Appendix I. Geographically cohesive groups with high to moderate posterior probabilities are identified at the right side with vertical lines, and correspond to those indicated in Fig. 3. Thick continuous lines indicate groups supported by high posterior probabilities (encircled values); dashed lines indicate groups supported by moderate posterior probabilities (within hexagons); and thin dotted lines indicate smaller posterior probabilities (within rectangles). Scale bar represents substitutions per site.

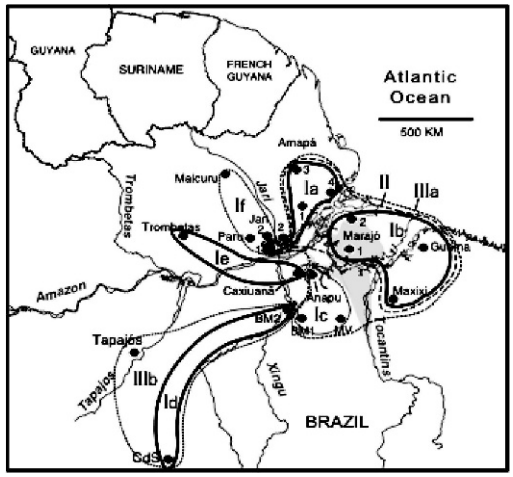

FIG. 3.—Samples of *Kentropyx calcarata* that were recovered in the 50% consensus Bayesian tree of concatenated *cyt b* and *16S* (Fig. 2). Groups surrounded by a continuous line are supported by 100% posterior probability; those surrounded by dashed lines are successively (from larger to smaller dashes to dots) less well-supported.

but again at a weaker level of support (P = 0.72 and 0.71, respectively; Fig. 2), and clade If is united with another locality north of the Amazon River (Amapa 2; Fig. 3). Note that clades Ie (partially) and If are both north of the Amazon River and are paraphyletic (or unresolved if we collapse the node with support <0.50) with respect to all clades south of the Amazon.

The ML mtDNA tree recovered clades Ib to If similar to the Bayesian tree (bootstrap values shown in Fig. 2; tree in supplemental material, Fig. S2; available online). However, most other relationships were quite different from the Bayesian analysis but were, overall, poorly supported. In spite of such differences, haplotypes north of the Amazon were still separated in two groups, one of which was basal to all remaining groups.

An AMOVA was performed considering the mtDNA tree obtained, so that the following "groups (populations)" were considered: Ia (Jari 1[a], Amapa 1, Amapa 3, Amapa 4), Ib (Maxixi, Marajo + Gunma), Ic (Anapu, Belo Monte 1, Monte Verde), Id + Tapajos (Castelo dos Sonhos + Belo Monte 2 as one population, Tapajos), Ie (Caxiuanã, Trombetas), and If (Jari 1[b], Jari 2, Maicuru, Paru). Variation within populations and among populations within groups was low, with most variation (~72%) between groups. This is in contrast with results obtained when populations are grouped geographically, considering the areas north of the Amazon, Marajó Island, west of and east of the Tocantins River, which represent the areas considered in our phylogenetic hypothesis (Fig. 1B). In this case, most variation (~64%) was partitioned among populations within groups, reflecting the artificial grouping (Table 1).

Gonatodes humeralis

In *G. humeralis* the combined *16S–cyt b* alignment had 1340 base-pairs (524 bp of *16S*, 816 bp of *cyt b*). Of the 56 samples analyzed, 44 distinct haplotypes were found and grouped into nine independent networks plus 18 isolated haplotypes when the connection limit was set at 95%, and 10 networks plus 14 isolated haplotypes when this limit was 90% (supplemental material, Fig. S3; available online). In both cases, each network connected only haplotypes from a single locality, except for Caxiuanã and Anapu at 90% connection limit. No haplotype appears in more than one locality.

Both the Bayesian (Fig. 4; ASDSF = 0.008; generation/–lnL plots leveled off at ~500,000 generations, with burn-in made at 1000 trees; mean and SE of combined runs = −5728.17 ± 0.15, ESS = 4574.89) and the ML (supplemental material Fig. S4, available online) trees show little support for relationships between areas. The only areas with well-supported links are Cametá and Tucuruí, both on the western margin of Tocantins River (clade Ic; P = 0.95), and (separately) the two localities in Amapá (clade Ia; P = 0.98) north of the Amazon and east of the Jari River. Caxiuanã and Anapu, separated by the Anapu River, are also recovered as a clade (Ib) but only with a moderate support (P = 0.81). Figure 5 visually summarizes these area relationships, which differ from those observed in *Kentropyx*, in which Caxiuanã is recovered as sister to Trombetas, on the opposite side of the Amazon River, and not to the geographically closer Anapu.

Because the phylogeographic analyses recovered a limited number of strongly supported clades, the AMOVA was performed only

TABLE 1.—Results of AMOVA in *K. calcarata*, considering (A) phylogenetic groups—the six main groups recovered by the phylogenetic analysis (Ia, Ib, Ic, Id + Tapajos, Ie, and If, as indicated in the text and in Fig. 2); (B) geographic groups—the four geographic areas (north of the Amazon, Marajó Island, west of Tocantins River, and east of the Tocantins River) we wanted to test.

Source of variation	df	Sum of components	Variance	Percentage of variation
A. Phylogenetic groups:				
Among groups	5	703.65	12.32 Va	70.39
Among populations within groups	13	155.19	2.84 Vb	16.22
Within populations	48	112.56	2.35 Vc	13.40
Total	66	971.40	17.51	
B. Geographic groups:				
Among groups	3	253.89	3.82 Va	22.20
Among populations within groups	15	604.96	11.04 Vb	64.17
Within populations	48	112.56	2.35 Vc	13.63
Total	66	971.541	17.21	

considering the four main geographic divisions: areas north of the Amazon (Amapá and northern Pará in Fig. 1), Marajó Island, west of Tocantins River, and east of Tocantins River. Results showed that the total variation for *G. humeralis* is larger than for *K. calcarata* data (Tables 2 and 3). However, we found a small variation both within populations and between groups, with most variation between populations within groups (Table 2), in agreement with previous analyses that showed distinct haplotypes in each locality. All analyses therefore point to populations of *G. humeralis* being highly differentiated and relatively isolated from each other, but analyses point to no geographic congruence with the area relationships being tested (Fig. 1).

Genetic Diversity and Demography

None of the species deviated significantly from the expectations of neutrality as indicated by nonsignificant Tajima's D and Fay and Wu's *Hs* values, implying overall population stability for both *K. calcarata* and *G. humeralis*. All estimates (θ_{sites}, $\theta_{sequence}$, haplotype and nucleotide diversity, and mean D_a) revealed substantially higher genetic diversity for *G. humeralis* than for *K. calcarata* (Table 3). Also, the effective population size of *G. humeralis* is about twice that of *K. calcarata*, indicating much deeper (ancient) coalescent times (Table 3). Regarding isolation-by-distance patterns, Mantel test results showed that genetic and geographic distances were weak ($r = 0.19$), but significantly correlated ($P = 0.04$; Table 3) in *K. calcarata*, but no significant correlation was found for *G. humeralis* (Table 3).

DISCUSSION

The two focal species revealed similar geographic patterns in that unique mtDNA haplotypes are largely restricted to single localities (with one exception in *K. calcarata*), yet the two species show very different phylogeographic structures. The phylogeographic structure of *G. humeralis* reflects a signature characteristic of extremely low-vagility species that display deep splits between localities. Such population structure is typical of many invertebrates (Bond et al., 2001; Hedin and Wood, 2002; Pfenniger and Posada, 2002), but it has been reported also in salamanders from Costa Rica (Garcia-Paris et al., 2000), in North American lizards of the *Xantusia vigilis* complex (Leavitt et al., 2007), and in the South American species *Phyllopezus pollicaris* (on-going research by FPW). Such a pattern may be caused by saturation of the gene regions sampled relative to the divergence history of this species, but it can also represent an artifact of overdispersed sampling relative to the demographic attributes of the organism (Templeton, 2004). We return to these issues again below.

On the other hand, *K. calcarata* shows a phylogeographic pattern marked by stronger geographical structure. Considering our hypothesis of area relationships based on recent geological studies, it is clear that the most recent separation event ("new Tocantins"; node 3 in Fig. 1B) is not detected in the *K. calcarata* genealogy; the most parsimonious explanation for this feature is the limited variation in our data relative to the recent age

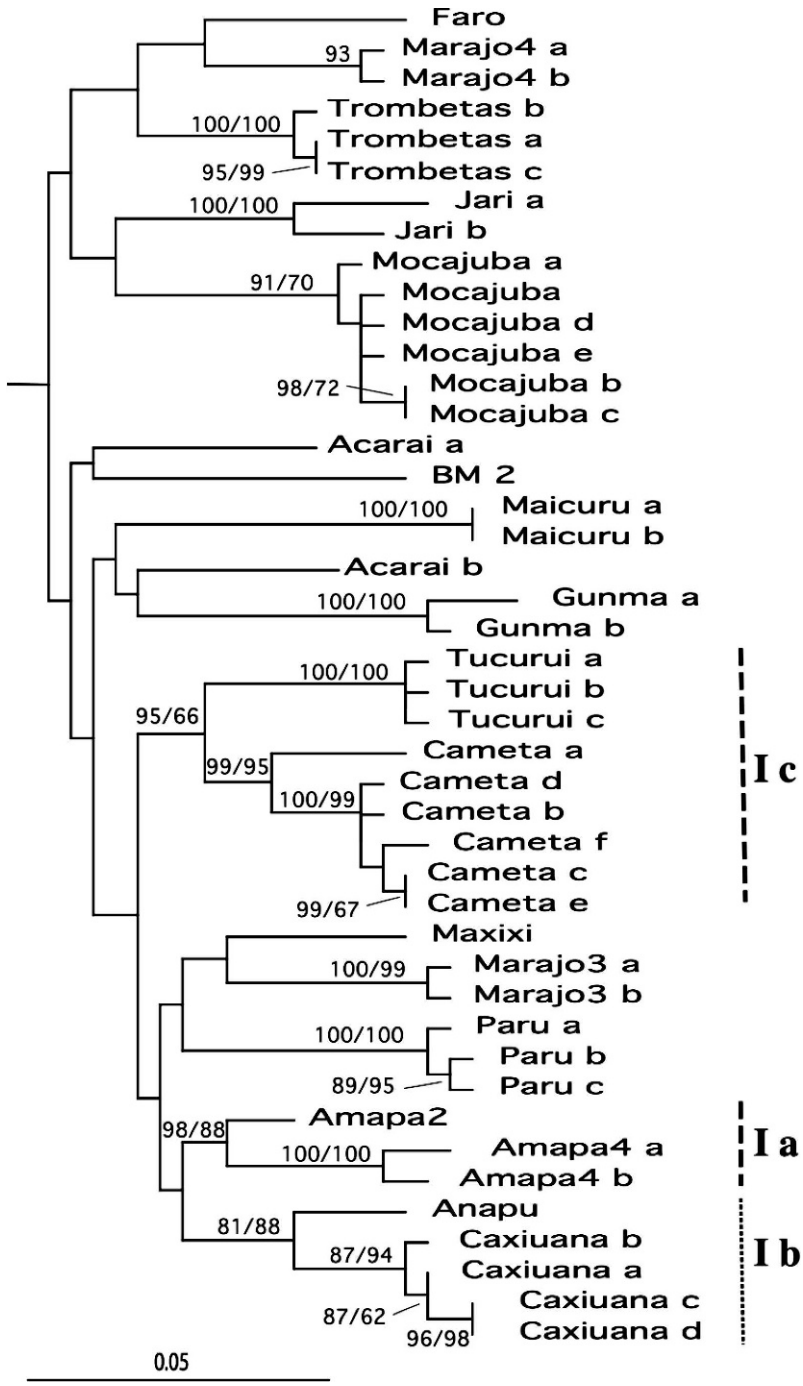

FIG. 4.—Bayesian consensus tree of concatenated *cyt b* and *16S* obtained for the samples of *Gonatodes humeralis*. Numbers at nodes represent posterior probabilities ≥70%/ML bootstrap values ≥50%. Haplotype terminals were replaced by their localities of origin followed by a letter (when more than one haplotype per locality) that identifies the specimen(s) with that haplotype in Appendix I. Locality names and groups shown at the right side correspond to those indicated in Fig. 5. Scale bar represents substitutions per site.

FIG. 5.—Studied populations of *Gonatodes humeralis* showing the only three pairs of localities (encircled by dashed lines) that were grouped with some support (81–98% posterior probability) according to the 50% consensus Bayesian tree of concatenated *cytochrome b* and *16S*. Larger dashes indicate groups with larger posterior probabilities.

of this event (6000–8000 yr BP; Rossetti and Valeriano, 2007). However, some deeper nodes in the phylogeographic history of *K. calcarata* are, in part, congruent with the area relationships predicted from the geological data. This partial congruence could explain the low, but significant, correlation between genetic and geographic distances found. For example, the "paleo-Tocantins" event (node 2 in Fig. 1B) is consistent with the strong phylogeographic signal we recover for clade Ib, and at a deeper level, clade IIIa (even though it also includes the strongly supported clade north of the Amazon, Ia, Amapá + northern Pará). Clade IIIa suggests that the barrier formed by the paleo-Tocantins channel may have been temporally linked to a similar barrier on the north side of the main Amazon River channel, so that relationships in this region are dominated by recent north–south connections (Ia + Ib), with east–west relationships reflecting earlier splits (Ic + (Ia + Ib)). Ayres and Clutton-Brock (1992) showed that faunal similarity between both sides of the Amazon River is larger close to the mouth than upriver. In lizards, at least a few species (*Arthrosaura kockii*, *Leposoma guianense*, and *Tretioscincus agilis*) are mainly distributed north of the Amazon but occur south of it east of the Xingu River (Avila-Pires, 1995), which also points to an earlier connection between the north and south sides of the Amazon close to its mouth. How this happened, however, remains unclear. Rearrangement of land masses might be part of the explanation for these similarities, perhaps as a consequence of tectonic movements such as those that eventually changed the course of the Tocantins River and created the Marajó Island (Rossetti and Góes, 2008; Rossetti et al., 2008). Such terrain movements are expected to occur mainly in meandering rivers, such as the Purus and the Juruá (Räsänen et al., 1987, 1990; Goulding et al., 2003), which is not the case of the Amazon. However, the Amazon River acquired its present shape and full sedimentation rate only at about 2.4 million years, with a long previous history of adjustments (Figueiredo et al., 2009). Although at the moment it is speculation, such terrain rearrangements may have occurred in this earlier phase.

Clade Ie ($P = 1.0$; Fig. 2), which includes populations on both sides of the Amazon River (Trombetas to the north, and Caxiuanã to the south of the Amazon and west of the Tocantins; Fig. 3), might have resulted from the same land rearrangements in the course of the Amazon River mentioned above, resulting in terrain transfer encompassing the lower Amazon and the Anapu rivers, such that an area previously north of the Amazon was shifted to the south bank. The alternative is

TABLE 2.—Results of AMOVA in *Gonatodes humeralis*, considering the four geographic areas (north of the Amazon, Marajó Island, west of Tocantins River, and east of the Tocantins River) that we wanted to test.

Source of variation	df	Sum of components	Variance (V)	Percentage of variation
Among groups	3	316.30	0.77 Va	3.22
Among populations within groups	13	795.73	20.03 Vb	83.27
Within populations	39	126.67	3.25 Vc	13.50
Total	55	1238.70	24.05	

TABLE 3.—Population genetic metrics estimated from mtDNA (*cyt b + 16S*) for *Kentropyx calcarata* and *Gonatodes humeralis* samples. *n* = sample size; θ = diversity parameter (per sequence); θ_{sites} = diversity parameter (θ per sites; lower and upper limits); Ne = effective population size; Hd = haplotype diversity (lower and upper limits); Π = nucleotide diversity per site (lower and upper limits); mean D_a = average net nucleotide differences across localities with more than two individuals sampled (minimum and maximum value); Tajima's D (*P*-value); *Hs* = Fay and Wu's *Hs* test of population expansion (*P*-value); and Mantel's corr. coef. (*P*-value). *P*-values in bold correspond to significant values at the 0.05 probability level. Ne was calculated assuming a mutation rate (μ) of 0.0065 substitutions per million years (Macey et al., 1998).

	n	θ	θ_{sites}	Ne	Hd	Π	Mean D_a	Tajima's D	*Hs*	Mantel's
K. calcarata	67	29.14	0.058	4.46×10^6	0.97	28.92	0.02	−0.11	0.18	0.19
		(18.28–46.24)	(0.04–0.09)		(0.94–0.98)	(11.36–65.61)	(0.001–0.04)	(0.44)	(0.32)	**(0.04)**
G. humeralis	56	45.201	0.133	10.23×10^6	0.98	45.2	0.03	−0.09	−0.46	−0.36
		(28.16–72.01)	(0.09–0.20)		(0.96–0.99)	(17.70–101.33)	(0.02–0.04)	(0.34)	(0.34)	(0.93)

that lizards have occasionally crossed the main channel passively on floating meadows that became free. Such rafts are not uncommon in the Amazon River and could potentially carry animals downriver, even though to our knowledge no record exists in the literature of such transport. Given the facility with which lizards can raft long distances, including transoceanic colonizations (de Queiroz, 2005), this type of transfer would not be surprising. At a deeper level, the mtDNA tree offers general support for isolation of many Amapá + northern Pará populations (clade If) from those south of the Amazon. This division corresponds to the most basal node of the hypothesized area cladogram in Fig. 1B.

The ML tree obtained for *K. calcarata* mtDNA, even if partially distinct from the Bayesian tree, also shows a split between areas east and west of the Tocantins River, and two groups north of the Amazon River. Contrary to the Bayesian tree, however, the eastern groups were basal to the western groups. Again the hypothesized area cladogram was partially recovered.

In *Gonatodes*, most of the high posterior probability values in the mtDNA tree support only haplotypes at single localities and show no support for the area cladogram hypothesized on basis of geologic data, which depicts the development of the lower Tocantins River–Marajó Island system. Our data indicate higher genetic diversity and ancient coalescent times for *G. humeralis;* therefore, it may be that saturation of gene regions has overwritten the geographic signal in our data, which would explain lack of correlation between genetic and geographic distances. Increased sampling density and inclusion of slower evolving nuclear markers will be important for an accurate assessment of the deeper phylogeographic structure (Leavitt et al., 2007), which might reflect the influence of much older geomorphological events than the recent events responsible for the development of the lower Tocantins River–Marajó Island system. The influence of ancient events that were not overwritten by the more recent events shown in Fig. 1 is, indeed, plausible considering the deep structure of the *G. humeralis* tree. Some events that were previously proposed as having a role in structuring

Amazonian populations and might have potentially shaped the deep structure of *G. humeralis* populations include ancient geological arches (one of the arches passes right by the Marajó basin, the Gurupá Arch), and the Miocene marine introgressions on the Amazon basin. However, these hypotheses also received criticism (Wesselingh and Salo, 2006), and should be considered as speculative at this point. Denser sampling (in terms of geographic coverage, number of individuals, and populations) is required to investigate such scenarios, and our results for *G. humeralis* should be seen as preliminary.

Given its biodiversity, size, and extremely complex geological and climatic history of Amazonia (Hoorn et al., 2010), we are encouraged by our results. Following some of the steps suggested by Buckley (2009: Fig. 1), both geographic and molecular sampling strategies can now be refined to provide more critical tests of the phylogeographic histories of both species. For example, additional geographic sampling will be needed for both species, but at different densities. *Kentropyx calcarata* is the larger and more active of the two species and likely has better dispersal capabilities (Avila-Pires, 1995; Vitt et al., 1997, 2000). In contrast, *G. humeralis* almost certainly has limited vagility or low dispersal distances and probably shorter generation times (Pianka and Vitt, 2003). Thus, local demes of *G. humeralis* will sort to monophyly for a given gene much faster than will demes of *K. calcarata,* and so geographic sampling density will need to be much higher for the former. Because deep splits in the mtDNA locus may develop despite gene flow between populations (Irwin, 2002; Kuo and Avise, 2005), sampling density must be scaled by dispersal distances and geographic continuity (or patchiness) of the target taxa (Templeton, 2004), as demonstrated by the studies of the North American "night lizards," *Xantusia* (Sinclair et al., 2004; Leavitt et al., 2007). It is also obvious that in both taxa, both more variable and less variable markers are needed to register the geologically youngest (node 3 in Fig. 1B) and the older events, and multiple nuclear markers now exist for extending lizard studies to multi-locus approaches (Benavides et al., 2009; Breitman et al., 2011).

In conclusion, although the *G. humeralis* phylogeographic structure shows no geographic congruence with the area relationships proposed to explain the development of the lower Tocantins River–Marajó Island system, we found signs of geographic congruence at the deeper nodes in the phylogeographic history of *K. calcarata*, a larger and more mobile lizard. Both species, however, showed low support at deeper levels, which indicates the need of further studies with additional markers and denser geographic and individual sampling. Although the results for the two species might look contradictory, differences in their biology and demographic histories partially explain the dissimilar patterns. The geomorphological events responsible for the establishment of the lower Tocantins River–Marajó Island in eastern Amazonia have therefore influenced, to some degree, the diversification history of associated biota at the regional scale. Further comparative phylogeographic studies, both focusing on specific regions and looking at the species' complete geographic range, will help to conciliate the conflicting patterns and bring light into the evolution of the Amazonian landscape.

Acknowledgments.—We thank Dilce de Fátima Rossetti for the original idea of such a project on the Marajó–Tocantins and for valuable discussions on the geology of the area; Arley Camargo for useful suggestions and help with some analyses; and those who contributed with tissue samples, without whose effort and extra time investment in the field this work would not have been possible. The study was financed in part by Fundação de Amparo à Pesquisa do Estado de São Paulo (FAPESP, process n° 2004/15518-6, awarded to D. F. Rossetti). TCSAP thanks CAPES for a postdoc scholarship (process n° 0093/09-2). DGM received a travel grant PCI-BEV from CNPq-MPEG (process n° 680.024/2008-5). FPW was supported by fellowships from CAPES/Fulbright (Coordenação de Aperfeiçoamento de Pessoal de Nível Superior; 15073722-2697/06-8) and by a graduate research assistantship from the BYU Department of Biology. Additional funding for lab work was provided by NSF-PIRE award (OISE 0530267; collaborative research on Patagonian Biodiversity) granted to the following institutions (listed alphabetically): Brigham Young University, Centro Nacional Patagónico (AR), Dalhousie University, Instituto Botánico Darwinion (AR), Universidad Austral de Chile, Universidad de Concepción, Universidad Nacional del Comahue, Universidad Nacional de Córdoba, and University of Nebraska.

Literature Cited

Aleixo, A. 2004. Historical diversification of a terra-firme forest bird superspecies: A phylogeographic perspective

on the role of different hypotheses of Amazonian diversification. Evolution 58:1303–1317.

Antonelli, A., A. Quijada-Mascareñas, A.J. Crawford, J.M. Bates, P.M. Velazco, and W. Wüster. 2010. Amazonian tetrapods and their relation to geological and climatic models. Pp. 386–404 in C. Hoorn and F.P. Wesselingh (Eds.), Amazonia, Landscape and Species Evolution: A Look into the Past. Wiley-Blackwell, UK.

Avila-Pires, T.C.S. 1995. Lizards of Brazilian Amazonia (Reptilia: Squamata). Zoologische Verhandelingen Leiden 299:1–706.

Ayres, J.M., and T.H. Clutton-Brock. 1992. River boundaries and species range size in Amazonian primates. American Naturalist 140:531–537.

Beerli, P., and M. Palczewski. 2010. Unified framework to evaluate panmixia and migration direction among multiple sampling locations. Genetics 185:313–326.

Benavides, E., R. Baum, H.M. Snell, H.L. Snell, and J.W. Sites, Jr. 2009. Island biogeography of Galapagos lava lizards (Tropiduridae: *Microlophus*): Species diversity and colonization of the archipelago. Evolution 63: 1606–1626.

Bond, J.E., M.C. Hedin, M.G. Ramirez, and B.D. Opell. 2001. Deep molecular divergence in the absence of morphological and ecological change in the California coastal dune endemic trapdoor spider *Aptostichus simus*. Molecular Ecology 10:899–910.

Breitman, M.F., L.J. Avila, J.W. Sites, Jr, and M. Morando. 2011. Lizards from the end of the world: Phylogenetic relationships of the *Liolaemus lineomaculatus* section (Squamata: Iguania: Liolaemini). Molecular Phylogenetics and Evolution 59:364–376.

Buckley, D. 2009. Toward an organismal, integrative, and iterative phylogeography. BioEssays 31:784–793.

Clement, M., D. Posada, and K.A. Crandall. 2000. TCS: A computer program to estimate gene genealogies. Molecular Ecology 9:1657–1660.

de Queiroz, A. 2005. The resurrection of oceanic dispersal in historical biogeography. Trends in Ecology and Evolution 20:68–73.

Eo, S.H., and A. DeWoody. 2011. Evolutionary rates of mitochondrial genomes correspond to diversification rates and to contemporary species richness in birds and reptiles. Proceedings of the Royal Society of London Series B-Biological Sciences 277:3587–3592.

Excoffier, L., G. Laval, and S. Schneider. 2005. Arlequin ver. 3.0: An integrated software package for population genetics data analysis. Evolutionary Bioinformatics Online 1:47–50.

Fay, J.C., and C.-I. Wu. 2000. Hitchhiking under positive Darwinian selection. Genetics 155:1405–1413.

Figueiredo, J., C. Hoorn, P. van der Ven, and E. Soares. 2009. Late Miocene onset of the Amazon River and the Amazon deep-sea fan: Evidence from the Foz do Amazonas Basin. Geology 37:619–622.

Fouquet, A., A. Gilles, M. Vences, C. Marty, M. Blanc, and N.J. Gemmell. 2007. Underestimation of species richness in Neotropical frogs revealed by mtDNA analyses. PLoS ONE 2 (10): e1109l DOI: 10.1371/journal.pone.0001109.

Gamble, T., A.M. Simons, G.R. Colli, and L.J. Vitt. 2008. Tertiary climate change and the diversification of the Amazonian gecko genus *Gonatodes* (Sphaerodactylidae, Squamata). Molecular Phylogenetics and Evolution 46:269–277.

Garcia-Paris, M., D.A. Good, G. Parra-Olea, and D.B. Wake. 2000. Biodiversity of Costa Rican salamanders: Implications of high levels of genetic differentiation and phylogeographic structure for species formation. Proceedings of the National Academy of Science 97:1640–1647.

Geurgas, S.R., and M.T. Rodrigues. 2009. The hidden diversity of *Coleodactylus amazonicus* (Sphaerodactylinae, Gekkota) revealed by molecular data. Molecular Phylogenetics and Evolution 54:583–593.

Goulding, M., R. Barthem, and E. Ferreira. 2003. The Smithsonian Atlas of the Amazon. Smithsonian Books, USA.

Guichenot, A. 1855. Animaux nouveaux ou rares recueillis pendant l'expédition dans les parties centrales de l'Amérique du Sud, de Rio de Janeiro à Lima, et de Lima au Pará exécutée par ordre du gouvernement français pendant les annés 1843 a 1847, sous la direction du Comte Francis de Castelnau. Tomes second. Bertrand, France.

Haffer, J. 1969. Speciation in Amazonian forest birds. Science 165:131–137.

Haffer, J. 1992. Ciclos de tempo e indicadores de tempos na história da Amazônia. Estudos Avançados 6 (15): 7–39.

Haffer, J. 2001. Hypotheses to explain the origin of species in Amazonia. Pp. 45–118 in I.C.G. Vieira, J.M.C. Silva, D.C. Oren, and M.A. D'Incao (Eds.), Diversidade Biológica e Cultural da Amazônia. Museu Paraense Emílio Goeldi, Brazil.

Hedin, M., and D.A. Wood. 2002. Genealogical exclusivity in geographically proximate populations of *Hypochilus thorelli* Marx (Araneae, Hypochilidae) on the Cumberland Plateau of North America. Molecular Ecology 11:1975–1988.

Hillis, D.M., and J.J. Bull. 1993. An empirical test of bootstrapping as a method for assessing confidence in phylogenetic analysis. Systematic Biology 42:182–192.

Hoorn, C., F.P. Wesselingh, H. ter Steege, M.A. Bermudez, A. Mora, J. Sevink, I. Sanmartín, A. Sanchez-Meseguer, C.L. Anderson, J.P. Figueiredo, C. Jaramillo, D. Riff, F.R. Negri, H. Hooghiemstra, J. Lundberg, T. Stadler, T. Särkinen, and A. Antonelli. 2010. Amazonia through time: Andean uplift, climate change, landscape evolution, and biodiversity. Science 330:927–931.

Irwin, D.E. 2002. Phylogenetic breaks without geographic barriers to gene flow. Evolution 56:2383–2394.

Jensen, J.L., A.J. Bohonak, and S.T. Kelley. 2005. Isolation by distance, web service. BMC Genetics 6:13. v.3.16 http://ibdws.sdsu.edu/.

Kuo, C.H., and J.C. Avise. 2005. Phylogeographic breaks in low-dispersal species: The emergence of concordance across gene trees. Genetica 124:179–186.

Latrubesse, E.M., M. Cozzuol, S.A.F. Silva-Caminha, C.A. Rigsby, M.L. Absy, and C. Jaramillo. 2010. The Late Miocene paleogeography of the Amazon Basin and the evolution of the Amazon River system. Earth-Science Reviews 99:99–124.

Leavitt, D.H., R.L. Bezy, K.A. Crandall, and J.W. Sites. 2007. Multi-locus DNA sequence data reveal a history of deep cryptic vicariance and habitat-driven

convergence in the desert night lizard *Xantusia vigilis* species complex (Squamata: Xantusiidae). Molecular Ecology 16:4455–4481.

Lomolino, M.V. 2004. Conservation biogeography. Pp. 292–296 in M.V. Lomolino and L.R. Heaney (Eds.), Frontiers of Biogeography. New Directions in the Geography of Nature. Sinauer Associates, USA.

Macey, J.R., J.A. Schulte, II, N.B. Ananjeva, A. Larson, N. Rastegar-Pouyani, S.M. Shammakov, and T.J. Papenfuss. 1998. Phylogenetic relationships among agamid lizards of the *Laudakia caucasia* species group: Testing hypotheses of biogeographic fragmentation and an area cladogram for the Iranian Plateau. Molecular Phylogenetics and Evolution 10:118–131.

Maddison, D.R., and W.P. Maddison. 2005. MacClade 4.08: Analysis of Phylogeny and Character Evolution. Sinauer Associates, Massachusetts, USA.

Mittermeier, R.A., C.G. Mittermeier, P.R. Gil, J. Pilgrim, G. Fonseca, T. Brooks, and W.R. Konstant (Eds.). 2003. Wilderness. Earth's Last Wild Places. University of Chicago Press, USA.

Moritz, C., J.L. Patton, C.J. Schneider, and T.B. Smith. 2000. Diversification of rainforest faunas: An integrated molecular approach. Annual Review of Ecology and Systematics 31:533–563.

Nogueira, C.C. 2006. Diversidade e Padrões de Distribuição da Fauna de Lagartos do Cerrado. Ph.D. Dissertation, Universidade de São Paulo, Brazil.

Pfenniger, M., and D. Posada. 2002. Phylogeographic history of the land snail *Candidula unifasciata* (Helicellinae, Stylommatophora): Fragmentation, corridor migration, and hybridization. Evolution 56:1776–1788.

Pianka, E.R., and L.J. Vitt. 2003. Lizards. Windows to the Evolution of Diversity. University of California Press, USA.

Posada, D., and K.A. Crandall. 1998. Modeltest: Testing the model of DNA substitution. Bioinformatics 14:817–818.

Rambaut, A., and A.J. Drummond. 2007. Tracer v.1.4. http://beast.bio.ed.ac.uk/Tracer.

Räsänen, M.E., J.S. Salo, and R.J. Kalliola. 1987. Fluvial perturbance in the western Amazon Basin: Regulation by long-term sub-Andean tectonics. Science 238: 1398–1401.

Räsänen, M.E., J.S. Salo, H. Jungnert, and L.R. Pittman. 1990. Evolution of the western Amazon lowland relief: Impact of Andean foreland dynamics. Terra Nova 2:320–332.

Rossetti, D.F., and A.M. Góes. 2008. Late Quaternary drainage dynamics in northern Brazil based on the study of a large paleochannel from southwestern Marajó Island. Anais da Academia Brasileira de Ciências 80:1–15.

Rossetti, D.F., and M.M. Valeriano. 2007. Evolution of the lowest Amazon basin modeled from the integration of geological and SRTM topographic data. Science Direct 70:253–265.

Rossetti, D.F., M.M. Valeriano, A.M. Góes, and M. Thales. 2008. Palaeodrainage on Marajó Island, northern Brazil, in relation to Holocene relative sea-level dynamics. The Holocene 18:1–12.

Rozas, J., J.C. Sánchez-DelBarrio, X. Messeguer, and R. Rozas. 2003. DnaSP, DNA polymorphism analyses by the coalescent and other methods. Bioinformatics 19:2496–2497.

Silva, J.M.C., A.B. Rylands, J.S. Silva, Jr, C. Gascon, and G.A.B. Fonseca. 2005. Primate diversity patterns and their conservation in Amazônia. Pp. 337–364 in A. Purvis, J.L. Gittleman, and T. Brooks (Eds.), Phylogeny and Conservation. Cambridge University Press, UK.

Silva, M.N.F., and J.L. Patton. 1998. Molecular phylogeography and the evolution and conservation of Amazonian mammals. Molecular Ecology 7:475–486.

Sinclair, E.A., R.L. Bezy, K. Bolles, J.L. Camarillo, K.A. Crandall, and J.W. Sites, Jr. 2004. Testing species boundaries in an ancient species complex with deep phylogeographic history: Genus *Xantusia* (Squamata: Xantusiidae). American Naturalist 164:396–414.

Spix, J.B. von. 1825. Animalia nova sive Species novae lacertarum, quas in itinere per Brasiliam annis MDCCCXVII–MDCCCXX jussu et auspicius Maximiliani Josephi J. Bavariae Regis suscepto collegit et descripsit Dr. J. B. de Spix. T. O. Weigel, Germany.

Stamatakis, A., T. Ludwig, and H. Meier. 2005. RAxML-III: A fast program for maximum likelihood-based inference of large phylogenetic trees. Bioinformatics 21:456–463.

Stamatakis, A., P. Hoover, and J. Rougemont. 2008. A fast bootstrapping algorithm for the RAxML web-servers. Systematic Biology 57:758–771.

Swofford, D.L. 2000. PAUP*: Phylogenetic Analysis Using Parsimony (*and Other Methods), Version 4.0b10. Sinauer Associates, Massachusetts, USA.

Tajima, F. 1996. The amount of DNA polymorphism maintained in a finite population when the neutral mutation rate varies among sites. Genetics 143:1457–1465.

Templeton, A.R. 2004. Statistical phylogeography: Methods of evaluating and minimizing inference errors. Molecular Ecology 13:789–809.

Vanzolini, P.E., and E.E. Williams. 1970. South American anoles: Geographic differentiation and evolution of the *Anolis chrysolepis* species groups (Sauria, Iguanidae). Arquivos do Museu de Zoologia São Paulo 19:1–298.

Vitt, L.J., P.A. Zani, and C.M. Lima. 1997. Heliotherms in tropical rain forest: The ecology of *Kentropyx calcarata* (Teiidae) and *Mabuya nigropunctata* (Scincidae) in the Curuá-Una of Brazil. Journal of Tropical Ecology 13: 199–220.

Vitt, L.J., R.A. Souza, S.S. Sartorius, T.C.S. Avila-Pires, and M.C. Espósito. 2000. Comparative ecology of sympatric *Gonatodes* (Squamata: Gekkonidae) in the western Amazon of Brazil. Copeia 2000:83–95.

Wallace, A.R. 1852. On the monkeys of the Amazon. Proceedings of the Zoological Society of London 20:107–110.

Werneck, F.P., L.G. Giugliano, R.G. Collevatti, and G.R. Colli. 2009. Phylogeny, biogeography and evolution of clutch size in South American lizards of the genus *Kentropyx* (Squamata: Teiidae). Molecular Ecology 18:262–278.

Wesselingh, F.P., and J.A. Salo. 2006. A Miocene perspective on the evolution of the Amazonian biota. Scripta Geologica 133:439–458.

Wesselingh, F.P., C. Hoorn, S.B. Kroonenberg, A. Antonelli, J.G. Lundberg, H.B. Vonhof, and H. Hooghiemstra. 2010.

On the origin of Amazonian landscapes and biodiversity: A synthesis. Pp. 421–431 in C. Hoorn and F. Wellelingh (Eds.), Amazonia: Landscape and Species Evolution: A Look into the Past. Wiley-Blackwell, UK.

Accepted: 4 February 2012
Associate Editor: Christopher Raxworthy

Appendix I

Specimens Examined, Map Localities, and Haplotypes

Names in parentheses refer to the mapped localities in Fig. 1. Letters a–f in parentheses after the catalog numbers refer to the haplotypes shown in Figs. 2 and 4. All geographic coordinates are based on the WGS84 datum.

Gonatodes humeralis: (Amapá 2) AP334: Brazil: Amapá: Laranjal do Jari: BR-156, N–NE of Laranjal do Jari, 0°43′48.2″S, 52°23′56.7″W. (Amapá 4) ACS3 (a), ACS35 (b): Brazil: Amapá: Macapá: Macapá and surroundings, 0°02′20″S, 51°07′45″W. (Jari 2) MPEG23199 (a), MSH7685 (b): Brazil: Pará: Almeirim: 20–40 km N–NW from Monte Dourado, 0°36′00″S, 52°41′00″W. (Paru) MPEG26665 (a), MPEG26667 (b), MPEG26668 (c), MPEG26669 (b): Brazil: Pará: Almeirim: FLOTA Paru, right margin Paru de Leste River, 0°56′30″S, 53°14′00″W. (Maicuru) MPEG26659 (a), MPEG26660 (b), MPEG26661 (a), MPEG26662 (a), MPEG26663 (a): Brazil: Pará: Almeirim: REBIO Maicuru, 0°49′00″N, 53°55′60″W. (Cametá) MPEG26803 (a), MPEG26809 (a), MPEG26806 (b), MPEG26810 (b), MPEG26811 (b), MPEG26814 (c), MPEG26817 (d), MPEG26820 (e), MPEG26833 (f): Brazil: Pará: Cametá: District Cametá, left margin Tocantins River, 2°15′40″S, 49°33′47″W. (Faro) MPEG26646, MPEG26651: Brazil: Pará: Faro: FLOTA Faro, 1°42′30″S, 57°12′20″W. (Mocajuba) MPEG26790 (a), MPEG26792 (b), MPEG26795 (c), MPEG26796 (d), MPEG26797 (e), one uncataloged specimen with broken tail: Brazil: Pará: Mocajuba: surroundings Mocajuba, right margins Tocantins River, 2°36′00″S, 49°28′30″W. (Trombetas) MPEG26634 (a), MPEG26635 (b), MPEG26638 (c): Brazil: Pará: Óbidos: FLOTA Trombetas, 0°57′45″S, 55°31′20″W. (Acarai) MPEG26653 (a), MPEG26654 (b): Brazil: Pará: Oriximiná: ESEC Grão Pará, Acarai Mountain, 1°17′00″N, 58°41′40″W. (Caxiuanã) GFM660 (a), GFM663 (b), MPEG25835 (c), MPEG25836 (d): Brazil: Pará: Portel: FLONA Caxiuanã, plot PPBIO and surroundings IBAMA post, 1°53′00″S, 51°33′00″W. (Anapu) GFM723: Brazil: Pará: Portel: right margin Anapu River (opposite to FLONA Caxiuanã), creeks Marinaú and Itapecuru, 1°51′40″S, 51°21′30″W. (Gunma) MPEG28021 (a), MPEG28023 (b), MPEG28024 (b): Brazil: Pará: Santa Bárbara: Parque Ecológico Gunma, 1°13′0.86″S, 48°17′41.2″W. (Marajó 4) TCAP3268 (a), TCAP3269 (b): Brazil: Pará: Santa Cruz do Arari: Ilha do Marajó, North Santa Cruz do Arari, west margin of Arari Lake, 0°27′57.7″S, 49°13′17.9″W. (Marajó 3) TCAP3189 (a), TCAP3194 (a), TCAP3197 (b), TCAP3201 (a), TCAP3202 (a): Brazil: Pará: Santa Cruz do Arari: Marajó Island, Vila Mocoons, 0°38′50.9″S, 49°27′57.8″W. (Maxixi) AAG868: Brazil: Pará: Tailândia: Maxixi Reserve, 2°58′44.9″S, 48°56′41.1″W. (Turucuí) MPEG24510 (a), MPEG24511 (b), MPEG24512 (c): Brazil: Pará: Tucuruí: APA Tucuruí, island in UHE Tucuruí lake reserve, 4°23′51″S, 49°34′13″W. (BM 2) MPEG25583: Brazil: Pará: Vitória do Xingu: Bom Jardim (left margin Xingu River), 3°24′45″S, 51°45′30″W.

Kentropyx calcarata: (Amapá 2) AP397 (a), AP412 (b), AP462 (c): Brazil: Amapá: Laranjal do Jari: BR-156, N–NE of Laranjal do Jari, 0°43′48.2″S, 52°23′56.7″W. (Amapá 4) ACS18 (a), ACS19 (a), ACS21 (b), ACS29 (b), ACS33 (b), ACS34 (c): Brazil: Amapá: Macapá: Macapá and surroundings, 0°02′20″S, 51°07′45″W. (Amapá 1) AP175 (a), AP240 (a), AP228 (b), AP285 (c): Brazil: Amapá: Mazagão: BR-156, N of Maracá, 0°09′2.7″S, 51°44′24.2″W. (Amapá 3) ACS41 (a), ACS52 (b), ACS58 (c), ACS60 (d): Brazil: Amapá: Serra do Navio, 0°52′07″S, 52°1′32.7″W. (Jari 2) MPEG23882 (a), MPEG23883 (a), MPEG23887 (b), MPEG23890 (a), MPEG23891 (c): Brazil: Pará: Almeirim: 20–40 km N–NW from Monte Dourado, 0°36′00″S, 52°41′00″W. (Jari 1) MPEG23878 (a), MPEG23885 (b), MPEG23889 (c), MPEG23894 (d): Brazil: Pará: Almeirim: Bituba and Quaruba, 1°07′00″S 52°47′00″W. (Paru) MPEG26727 (a), MPEG26730 (b), MPEG26731 (b), MPEG26738 (c), MPEG26747 (d), MPEG26769 (b), MPEG26775 (e): Brazil: Pará: Almeirim: FLOTA Paru, right margin Paru de Leste River, 0°56′30″S, 53°14′00″W. (Maicuru) MPEG26694 (a), MPEG26700 (a), MPEG26703 (b), MPEG26706 (c), MPEG26708 (d), MPEG26716 (d), MPEG26721 (e): Brazil: Pará: Almeirim: REBIO Maicuru, 0°49′00″N, 53°55′60″W. (CdS) MPEG28522 (a), MPEG28525 (b): Brazil: Pará: Altamira: BR-163, E Castelo de Sonhos, 940 km N of Cuiabá, 8°13′3.24″S, 55°0′57.4″W. (BM 1) MPEG24833 (a), MPEG24845 (b): Brazil: Pará: Anapu: Caracol (right margin Xingu River), 3°27′30″S, 51°39′24″W. (Marajó 2) MJH32 (a), MJH44 (b), MJH52 (c), MJH62 (b), MJH64 (a): Brazil: Pará: Chaves: Marajó Island, Fazenda Tauari, lower Cururu River, 0°25′00″S, 49°58′00″W. (Marajó 1) TCAP3376: Brazil: Pará: Curralinho: Marajó Island, trail Breves-Anajás, 1°27′00″S, 50°23′00″W. (Tapajós) MPEG22297: Brazil: Pará: Itaituba: PARNA Amazônia: left margin Tapajós River, 04°40′26.5″S, 56°32′52″W. (Trombetas) MPEG26684 (a), MPEG26685 (b), MPEG26687 (c), MPEG26689 (d), MPEG26690 (e): Brazil: Pará: Óbidos: FLOTA Trombetas, 0°57′45″S, 55°31′20″W. (MV) MPEG24691: Brazil: Pará: Portel: Fazenda Riacho Monte Verde (Precious Woods Pará), area 2001a, 3°23′02″S, 50°27′27″W. (Caxiuanã) MPEG25851 (b), MPEG25852 (a), MPEG25870 (b), MPEG26328 (c): Brazil: Pará: Portel: FLONA Caxiuanã, plot PPBIO and surroundings IBAMA post, 1°53′00″S, 51°33′00″W. (Anapu) GFM764: Brazil: Pará: Portel: right margin Anapu River (opposite to FLONA Caxiuanã), creeks Marinaú and Itapecuru, 1°51′40″S, 51°21′30″W. (Gunma) MPEG28013: Brazil: Pará: Santa Bárbara: Parque Ecológico Gunma, 1°13′0.86″S, 48°17′41.2″W. (Maxixi) AAG864 (a), AAG865 (b): Brazil: Pará: Tailândia: Maxixi Reserve, 2°58′44.9″S; 48°56′41.1″W. (BM 2) MPEG24827, MPEG24836: Brazil: Pará: Vitória do Xingu: Bom Jardim (left margin Xingu River), 3°24′45″S, 51°45′30″W.